JOURNAL OF Applied Polymer SCIENCE

Isothermal Crystallization and Spherulite Growth Behavior of Stereo Multiblock Poly(lactic acid)s: Effects of Block Length

Md. Hafezur Rahaman, Hideto Tsuji
Department of Environmental and Life Sciences, Graduate School of Engineering, Toyohashi University of Technology, Tempaku-cho, Toyohashi, Aichi 441-8580, Japan
Correspondence to: H. Tsuji (E-mail: tsuji@ens.tut.ac.jp)

ABSTRACT: Stereo multiblock poly(lactic acid)s (PLA)s and stereo diblock poly(lactic acid) (DB) with a wide variety of block length of 15.4–61.9 lactyl units are synthesized, and the effects of block length sequence on crystallization and spherulite growth behavior are investigated at different crystallization temperatures, in comparison with neat poly(L-lactide) (PLLA), poly(D-lactide) (PDLA), and PLLA/PDLA blend. Only stereocomplex crystallites as crystalline species are formed in the stereo multiblock PLAs and DB, irrespective of block length and crystallization temperature. The maximum crystallinities (33–61%), maximum radial growth rate of spherulites (0.7–56.7 μm min^{-1}), and equilibrium melting temperatures (182.0–216.5°C) increased with increasing block length but are less than those of PLLA/PDLA blend (67 %, 122.5 μm min^{-1}, and 246.0°C). The spherulite growth rates and overall crystallization rates of the stereo multiblock PLAs and DB increased with increasing block length and are lower than that of PLLA/PDLA blend. © 2013 Wiley Periodicals, Inc. J. Appl. Polym. Sci. 000: 000–000, 2013

KEYWORDS: copolymer; crystallization; biopolymers; renewable polymers

Received 10 September 2012; accepted 20 December 2012; published online
DOI: 10.1002/app.38953

INTRODUCTION

Poly(L-lactic acid) (PLLA), a plant-derived polyester, has found applications in the biomedical and packaging fields because of its biodegradability and biocompatibility.[1–4] Intensive research is going on to improve the properties of PLLA as an alternative to petro-derived polymers to reduce the environmental impact.[5–9] Until now poly(lactic acid) (PLA) has enjoyed little success in replacing petroleum-based plastics in the applications which require high impact strength and thermal stability. The mechanical and thermal properties and biodegradability of a semicrystalline polymer generally depend on the crystalline structure and crystallinity.[10] The stereocomplex crystallization between PLLA and poly(D-lactic acid) (PDLA) improves mechanical and thermal properties of PLA-based materials.[11–14] However, stereocomplex crystallization is disturbed when high-molecular weight PLLA and PDLA are used because of the difficulty in molecular level mixing. A promising method for obtaining stereocomplexed PLA is to use stereoblock PLA composed of PLLA and PDLA segments. Because of neighboring effects of the PLLA and PDLA blocks, stereoblock PLA readily forms stereocomplex crystallites in a wide range of processing windows. The crystallization behavior of block copolymers has been an active area of research for the past several decades. In 1990, Yui et al.[15] first showed that stereocomplex crystallization occurs in diblock copolymers PLLA-*b*-PDLA. To know the crystallization mechanism in details, stereocomplex crystallization behavior of diblock or triblcok PLA and blend, that is, spherulite formation, isothermal crystallization kinetics, and regime analyses of these polymers[16–20] and also the crystallization and morphology of diblock copolymers with one crystallizable block[21,22] have been investigated extensively. Tsuji et al.[17] showed that only stereocomplex crystallities as crystalline species were formed in PLLA-*b*-PDLA copolymers with M_n of 3.9 $\times$ 10^3–1.1 $\times$ 10^4 g mol^{-1}. Also, crystallization and stereocomplexation behavior of diblock copolymers which contained a crystalline block and a amorphous block, that is PLLA- or PDLA-poly(*N*,*N*-dimethylamino-2-ethylmethacrylate) (PDMAEMA) has been reported by Michell et al.[21] They concluded that the crystallization kinetics of the PLLA or PDLA blocks were retarded by the presence of amorphous PDMAEMA block and PLLA-*b*-PDMAEMA/PDLA-*b*-PDMAEMA blend formed stereocomplex crystallites.

In a previous study, we have shown that only stereocomplex crystallization also takes place in stereo multiblock PLA copolymers with average block length (v_{av}) higher than 7 lactyl units.[23] However, as far as we are aware, stereocomplex crystallization of stereo multiblock PLA copolymers consisting of relatively short PLLA and PDLA segments has not been reported. In this study, crystallization and spherulite growth behavior of stereo

Table I. Molecular Characteristics of Prepolymers and Blends Used to Synthesize Stereo Multiblock PLAs

Prepolymer				Blend					
Code	Mon./Coin.[a]	M_w[b] [g mol^{-1}]	M_w/M_n[c]	Code	M_w [g mol^{-1}]	M_w/M_n	T_m[d] [°C]	$[\alpha]^{25}_{589}$[e] [° dm^{-1} g^{-1} cm^3]	L-lactyl unit content [%]
L12	12.0	2.24×10^3	3.85	L12/D12	2.25×10^3	1.76	218.5	−1.0	50.3
D12	12.0	2.02×10^3	4.85						
L14	13.5	2.46×10^3	2.29	L14/D14	3.14×10^3	1.93	223.6	1.0	49.7
D14	13.5	2.32×10^3	2.16						
L15	14.5	5.50×10^3	7.48	L15/D15	5.16×10^3	1.54	229.9	0.8	49.8
D15	14.5	4.52×10^3	6.79						

[a]Ratio of monomer to coinitiator; [b]Weight-average molecular weight; [c]Number-average molecular weight; [d]Melting temperature; [e]Specific optical rotation in a mixture of chloroform (95 vol %) and 1,1,1,3,3,3-hexafluoro-2-propanol (5 vol %) at 589 nm and 25°C.

multiblock PLAs with various stereoblock lengths were investigated using wide-angle X-ray scattering (WAXS), differential scanning calorimetry (DSC), and polarized optical microscopy (POM).

EXPERIMENTAL

Materials and methods

Stereo multiblock PLAs were synthesized as reported previously.[23] Low-molecular weight PLLA and PDLA prepolymers were synthesized by ring-opening polymerization of L- and D-lactide (assay 99.5%, Purac Biochem, Gorinchem, The Netherlands) in the presence of stannous octoate (0.03 wt % of lactide) as the initiator with L- and D-lactic acids as the coinitiators, respectively, at 140°C for 10 h.[24] Thus, synthesized PLLA and PDLA prepolymers are abbreviated as L and D with monomer/coinitiator ratio (mol/mol), respectively (Table I). Blends utilized for the synthesis of stereo multiblock PLAs were prepared by casting the equimolar mixture of separately prepared solutions of PLLA and PDLA (5 g dL^{-1}), solvent evaporation at 25°C for approximately 3 days, and drying under reduced pressure for 7 days.[25] To remove low-molecular weight oligomers and monomers from the blends, these blends were extracted with methanol, followed by drying in reduced pressure for 7 days. Here, the pairs of PLLA and PDLA prepolymers used for blend preparation were synthesized with the identical monomer/coinitiator ratios. The blends are abbreviated as PLLA/PDLA prepolymers code used for blend preparation (Table I).

For the synthesis of stereo multiblock PLAs, melt-polycondensation of these blends were performed in the presence of *p*-toluenesulfonic acid monohydrate (Nacalai Tesque, Kyoto, Japan, 5

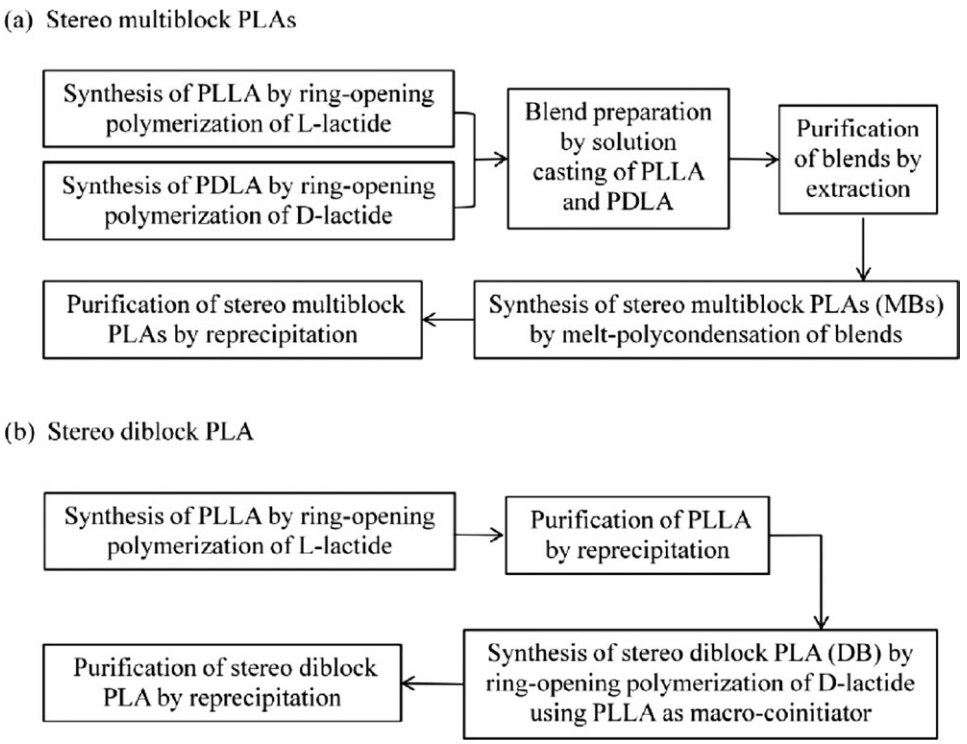

Scheme 1. Schematic flow diagram of synthesis of stereo multiblock PLAs (MBs) (a) and diblock PLA (DB) (b).

Table II. Molecular Characteristics of Synthesized Polymers and Blend

Code	M_w[a] [g mol^{-1}]	M_w/M_n[b]	$[\alpha]^{25}_{589}$[c] [° dm^{-1} g^{-1} cm^3]	*L*-lactyl unit content [%]
MB12	1.25×10^4	1.67	−0.8	50.3
MB14	1.22×10^4	1.68	−0.5	50.2
MB15	1.52×10^4	1.88	1.0	49.7
DB	1.39×10^4	1.86	−3.3	51.0
L62P	1.27×10^4	1.50	−160.0	100.0
D62P	1.17×10^4	1.49	158.0	0.6
L62P/D62P	1.27×10^4	1.62	0.0	50.0

[a]Weight-average molecular weight; [b]Number-average molecular weight; [c]Specific optical rotation in a mixture of chloroform (95 vol %) and 1,1,1,3,3,3-hexafluoro-2-propanol (5 vol %) at 589 nm and 25°C.

wt %) as the catalyst at 200°C under reduced pressure (1.3 kPa) and constant nitrogen gas flow.[23] Before polycondensation, the L12/D12 and L14/D14 blends and the L15/D15 blend were melted at 235 and 240°C, respectively, for 10 min under atmospheric pressure and constant nitrogen gas flow, then the temperature was decreased to 200°C and the pressure was decreased to 1.3 kPa. The latter high temperature of 240°C for the L15/D15 blend was due to its high melting temperature (T_m) = 230°C. Synthesized stereo multiblock PLAs were purified with the mixture of chloroform (95 vol %) and 1,1,1,3,3,3-hexafluoro-2-propanol (Nacalai Tesque, Kyoto, Japan) (5 vol %) as the solvent and methanol as the nonsolvent to remove low-molecular weight oligomers and monomers, and then dried under reduced pressure for 7 days. Synthesized stereo multiblock PLAs are abbreviated as MB with numerical code of prepolymers (the blends for the synthesis of stereo multiblock PLAs were prepared from PLLA and PDLA of the identical numerical codes, i.e., similar molecular weights).

As a reference, a stereo diblock PLA was synthesized according to the procedure reported by Yui et al.[15] Ring opening polymerization of D-lactide was performed in toluene in the presence of PLLA [weight-average molecular weight (M_w) of 7.01×10^3 g mol^{-1}] [PLLA/D-lactide (w/w) = 1/1] and stannous octoate (0.3 wt% of D-lactide) at 120°C for 24 h after sealing in a test tube. Thus obtained copolymer, which became insoluble in toluene at room temperature, was removed from toluene, dissolve in a mixed solvent of chloroform (95 vol %) and 1,1,1,3,3,3-hexafluoro-2-propanol (5 vol %), and then precipitated in methanol and abbreviated as DB. Scheme 1 shows the schematic flow diagram of synthesis of stereo multiblock PLAs and diblock PLA. Reference PLLA and PDLA with the molecular weights similar to those of

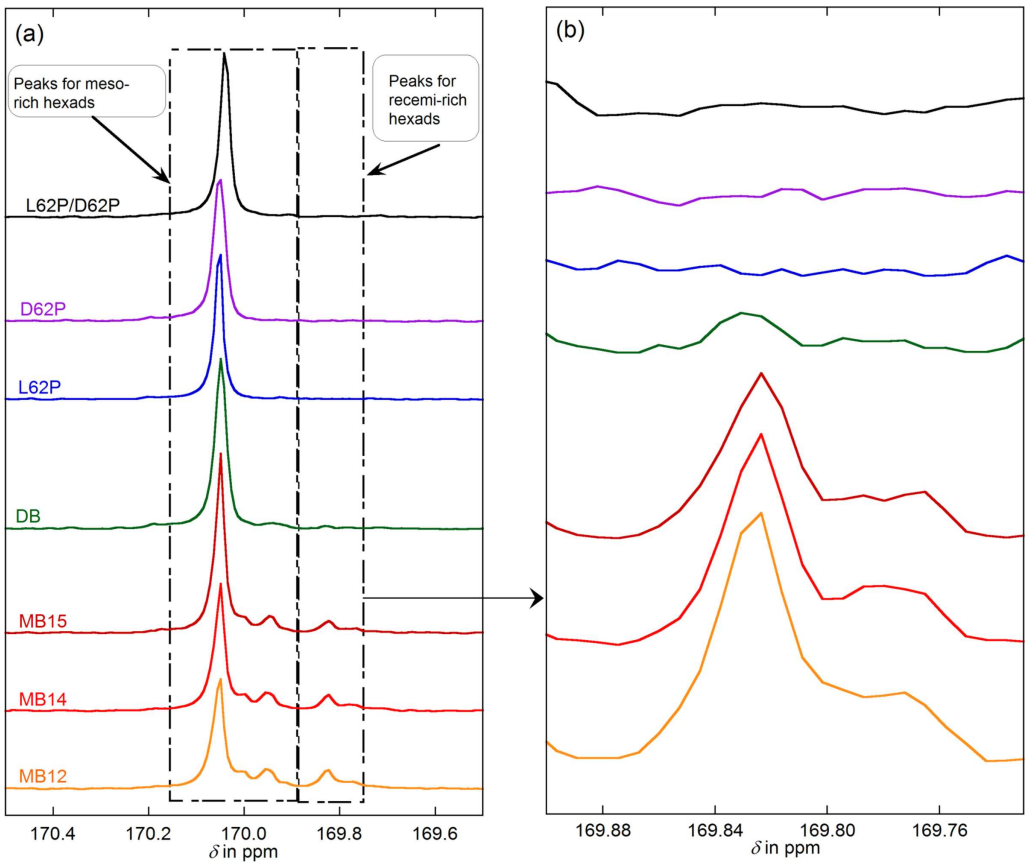

Figure 1. ^{13}C NMR spectra of the carbonyl region of synthesized polymers and blend (a) and enlarged recemi-rich hexads peak area (b). [Color figure can be viewed in the online issue, which is available at wileyonlinelibrary.com.]

Table III. The Average Block Lengths (ν_{av}s) of Stereo Multiblock PLAs (MB12, Mb14, and Mb15) and Stereo Diblock PLA (DB) Estimated from Carbonyl Region of ^{13}C NMR Spectra

Code	$I_{i,ii}$[a] [mmmmm, mmmmr, rmmmm, rmmmr]	I_{iii}[b] [mmmrm, mrmmm, rmrmm, mmrmr, mmrmm, rmrmr, mrmrm]	P_m[c]	P_r[d]	ν_{av}[e]
MB12	0.8180	0.1820	0.9352	0.0648	15.4
MB14	0.8430	0.1570	0.9447	0.0553	18.1
MB15	0.8915	0.1085	0.9624	0.0376	26.6
DB	0.9523	0.0477	0.9838	0.0162	61.9

[a]Area of isotactic and relatively isotactic peaks; [b]Area of relatively syndiotacitc peaks; [c]Probability of forming meso (m) diad; [d]Probability of forming recemic (r) diad; [e]Average block length of the L- or D- units of stereoblock PLAs.

stereo multiblock PLAs were synthesized by the same procedure with that utilized for the PLLA and PDLA prepolymers, and purified with chloroform and methanol as the solvent and nonsolvent, respectively. They are abbreviated by the same procedure with that used for the prepolymers (Table I). P was added to the abbreviations because they were purified before blend preparation. A blend was prepared from these PLLA and PDLA by the aforementioned procedure for further reference. Table II shows the molecular characteristics of the synthesized polymers and blend.

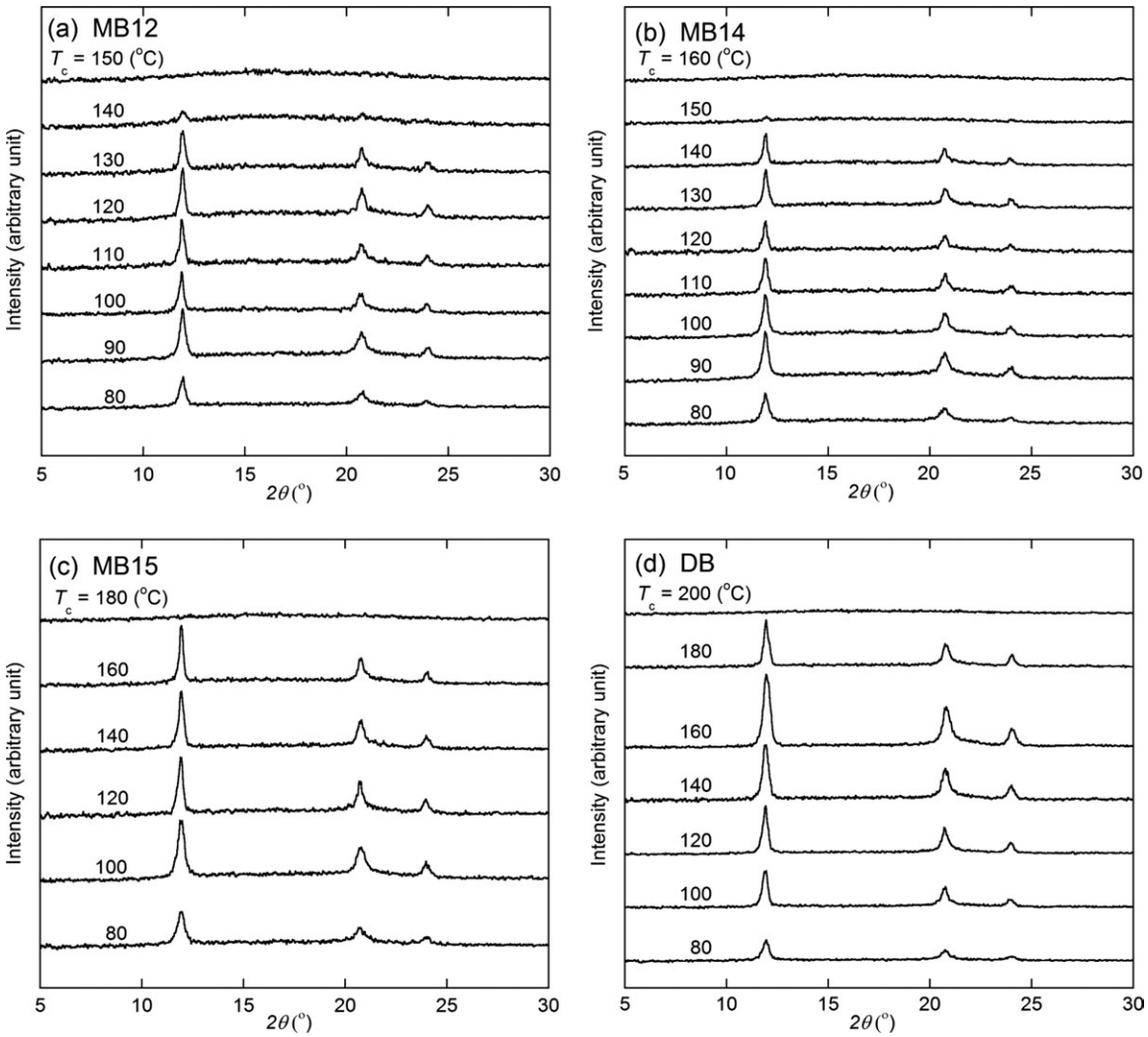

Figure 2. WAXS profiles of polymers and blend isothermally crystallized from the melt at different T_cs.

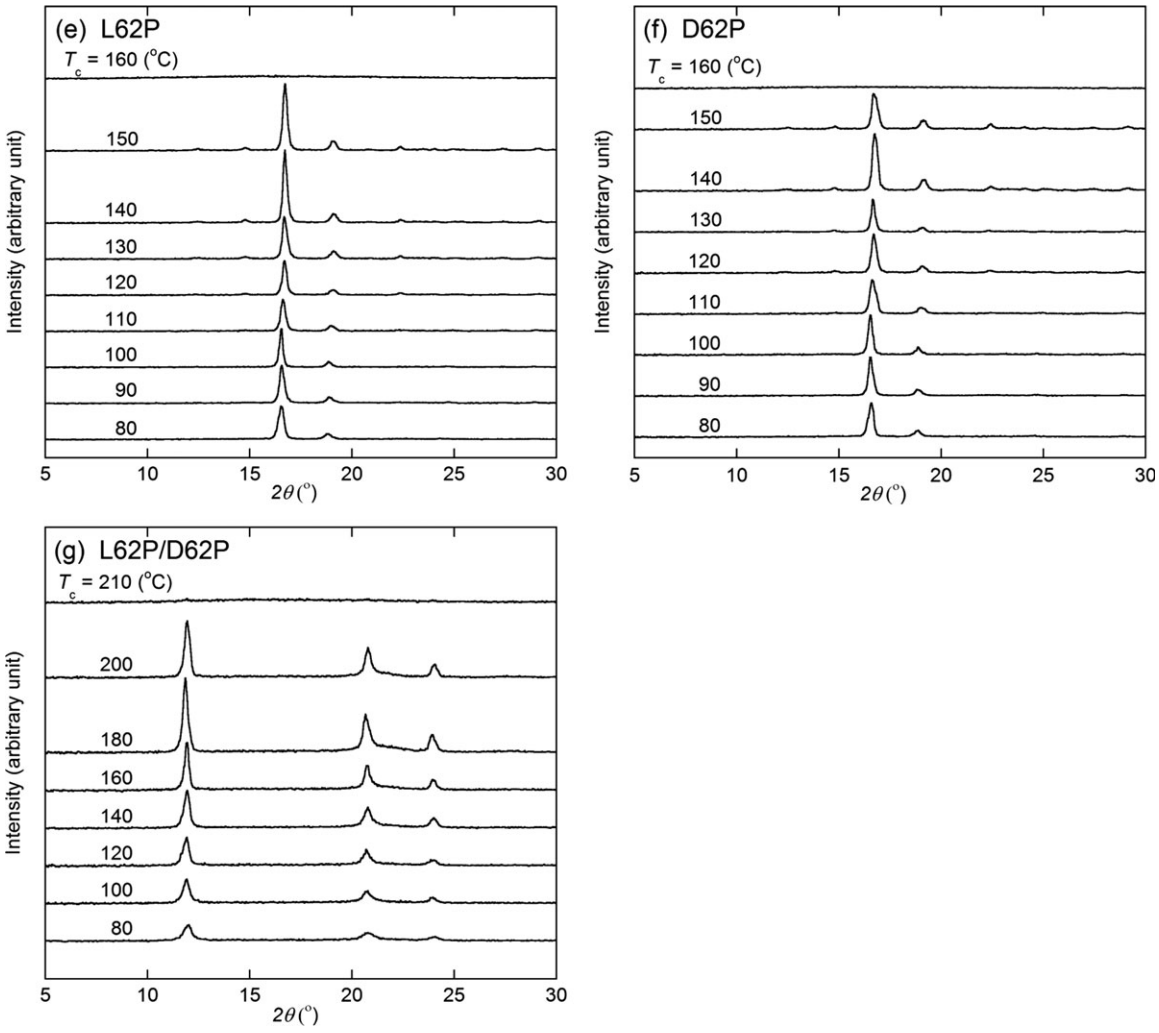

Figure 2. (*Continued*).

For the preparation of crystallized specimens, about 3 mg of synthesized and purified polymers and blend were taken in a DSC pan and sealed in a test tube under reduced pressure, melted at 250°C for 3 min, crystallized at different T_c values for 10 h and quenched with iced water at 0°C for 5 min. Thus, prepared isothermally crystallized specimens were used for further DSC and WAXS measurements.

Measurements

The weight- and number-average molecular weight (M_w and M_n, respectively) of the synthesized polymers and blends were evaluated in chloroform at 40°C using a Tosoh (Tokyo, Japan) GPC system (refractive-index monitor: RI-8020) with two TSK gel columns (GMH_{XL}) and polystyrene standards. Therefore, the molecular weights are those relative to polystyrene. For the preparation of GPC sample solutions of the blends, and stereoblock PLAs, mixture of chloroform and 1,1,1,3,3,3-hexafluoro-2-propanol (5 vol.%) was used as the solvent, whereas in the cases of PLLA and PDLA homopolymers, only chloroform was used as the solvent. The specific optical rotation values of the blends and synthesized polymers were measured in aforementioned mixed solvent at a concentration of 1 g dL^{-1} and 25°C using a JASCO (Tokyo, Japan) P-2100 polarimeter at a wave length of 589 nm. The L-lactyl unit contents of the specimens were estimated by the following equation:

$$\text{L-lactyl unit content (\%)} = 100\{[\alpha]_{25}^{589} + [\alpha]_{25}^{589}(\text{PLLA})\}/\{2\,[\alpha]_{25}^{589}(\text{PLLA})\}$$

where $[\alpha]_{25}^{589}(\text{PLLA})$ is the $[\alpha]_{25}^{589}$ values for the PLLA homopolymer. The evaluated molecular characteristics of synthesized polymers and blends are shown in Tables I and II. 100 MHz ^{13}C NMR spectra were obtained with a Bruker Biospin (MA, USA) AVANCE II 400, spectrometer in deuterated chloroform (99.8 atom %) containing 1 vol % tetramethylsilane (Sigma-Aldrich, St. Louis, MO) as the internal reference, which was added with 1,1,1,3,3,3-hexafluoro-2-propanol (5 vol %).

The thermal properties of isothermally crystallized specimens were determined by a Shimadzu (Kyoto, Japan) DSC-50

Applied Polymer SCIENCE

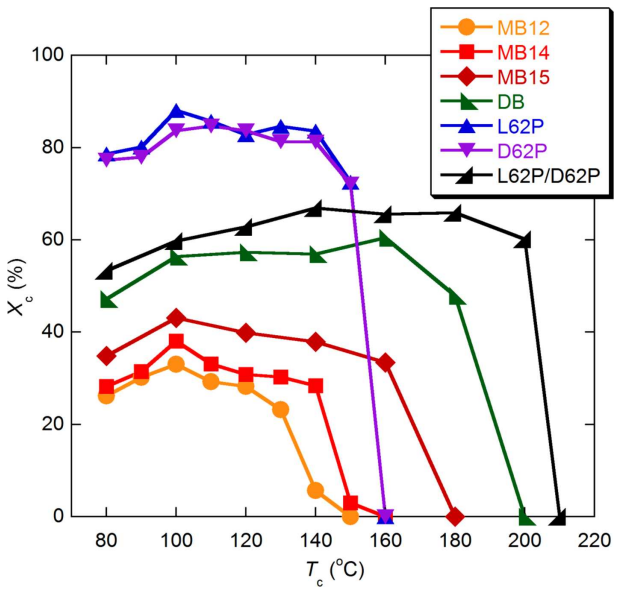

Figure 3. Crystallinity (X_c) of polymers and blend isothermally crystallized from the melt at different T_cs. [Color figure can be viewed in the online issue, which is available at wileyonlinelibrary.com.]

differential scanning calorimeter under a nitrogen gas flow of 50 mL min^{-1} at a heating rate of 10°C min^{-1}. The WAXS measurements of isothermally crystallized specimens were performed at 25°C using a Rigaku (Tokyo, Japan) RINT-2500 equipped with a Cu-K_α source ($\lambda = 0.15418$ nm) in a 2θ range of 5–35° at a scan rate of 4° min^{-1}, which operated at 40 kV and 200 mA. The crystallinity (X_c) values of these specimens were estimated from the WAXS measurements using the following equation:

$$X_c\ (\%) = 100\ S_c/(S_c + S_a), \tag{2}$$

where S_c and S_a are crystalline and amorphous diffraction peak areas, respectively. We did not calculate crystallinity from DSC results, because stereocomplex crystallites are formed during DSC heating, as reported previously.[26] The spherulite growth in the specimens during isothermal crystallization was observed by an Olympus (Tokyo, Japan) polarized optical microscope (BX50) equipped with a heating-cooling stage and temperature controller (LK-600PM, Linkam Scientific Instruments, Surrey, UK) under a constant nitrogen gas flow. The specimens were first heated from room temperature to 250°C at 100°C min^{-1}, held at the same temperature for 3 min, cooled at a rate of −100°C min^{-1} to a crystallization temperature (T_c), and held at the same T_c (spherulite growth was observed here). The overall crystallization behavior of the specimens during isothermal crystallization was monitored by measuring the light intensity transmitted through the specimens using the polarized optical microscope (BX50) equipped with an As One (Osaka, Japan) LM-332 photometer.

RESULTS AND DISCUSSION

^{13}C NMR Spectroscopy

To estimate the distribution of L- and D-units of synthesized polymers and blend ^{13}C NMR measurements were performed. Figure 1 shows the ^{13}C NMR spectra of carbonyl region of synthesized polymers and blend. The average block length (ν_{av}) values of L- or D-units of the stereo multiblock PLAs were evaluated from the ^{13}C NMR spectra and the signal assignments of the hexads sequences reported previously by Fukushima et al.[27] As shown in Figure 1, the peak at 170.06 ppm (i) and the peaks in the range of 169.95–170.01 ppm (ii) are assigned to the meso diad (m)-rich hexads (mmmmm, mmmmr, rmmmm, rmmmr), while the peaks at around 169.83 ppm (iii) are assigned to the racemic diad (r)-rich hexads (mmmrm, mrmmm, rmrmm, mmrmr, mmrmm, rmrmr, mrmrm) that should be present in the linking segments of the PLLA and PDLA blocks.[27–29] Therefore, the appearance of the large peak (i) and the small peaks (ii) and (iii) are indicative of the blocky nature of the synthesized stereo multiblock PLAs (MB12, MB14, and MB15) and stereo diblock PLA (DB), whereas only the appearance of large peak (i) of homopolymers (L62P and D62P) and blend (L62P/D62P) indicate that these polymers do not contain any blocks, in consistent with the expectation from reported results.[27] From the areas of peaks (i) and (ii) and that of peaks (iii) relative to the total peak area ($I_{i,ii}$ and I_{iii}, respectively), ν_{av} of stereo multiblock PLAs can be evaluated assuming the ordinary Bernoullian statistics. When the probabilities of forming meso (m) diad and recemic (r) diad are represented by P_m and P_r, the ratios of the hexads can be calculated from their formation probabilities and related to the integral ratios as shown by eqs. (3) and (4):

$$I_{i,ii} = {P_m}^5 + 2{P_m}^4\ P_r + {P_m}^3\ {P_r}^2, \tag{3}$$

$$I_{iii} = 3{P_m}^4\ P_r + 3{P_m}^3\ {P_r}^2 + {P_m}^2\ {P_r}^3. \tag{4}$$

From the eqs. (3) and (4) together with the relations of $P_m + P_r = 1$ and $I_{i,ii}+I_{iii} = 1$, both P_m and P_r can be estimated from integral ratios $I_{i,ii}$ and I_{iii}. Finally, ν_{av} was calculated as $\nu_{av} = 1/P_r$. The ν_{av} values of stereo multiblock PLAs thus obtained are summarized in the Table III. The ν_{av} of the stereo multiblock PLAs increased with increasing the M_w of the blend used for their synthesis, in consistent with the expectation from our previous literature but higher than that from similar blend.[23] This may be due to the small change in reaction condition (reduced pressure from 1.6 to 1.3 kPa), which helps to increase the rate of removal of water which is formed by polycondensation, resulting in higher ν_{av}.

Wide-Angle X-ray Scattering

To estimate the crystalline species and X_c values of the specimens, WAXS measurements were performed. Figure 2 shows the WAXS profiles of the polymers and blend crystallized at different T_cs. MB12, MB14, MB15, DB, and L62P/D62P had crystalline diffraction peaks at 2θ values of around 12, 21, and 24°, indicating the formation of only stereocomplex crystallities as crystalline species.[11,16,30] On the other hand, the sharp crystalline peaks were observed at 2θ values of around 16° and 19° for L62P and D62P, indicating the formation of α- or α′- form homo-crystallites of PLLA.[31] The X_c values of these samples estimated from the WAXS profiles are plotted in Figure 3 as a function of T_c. The maximum X_c values of stereo multiblock

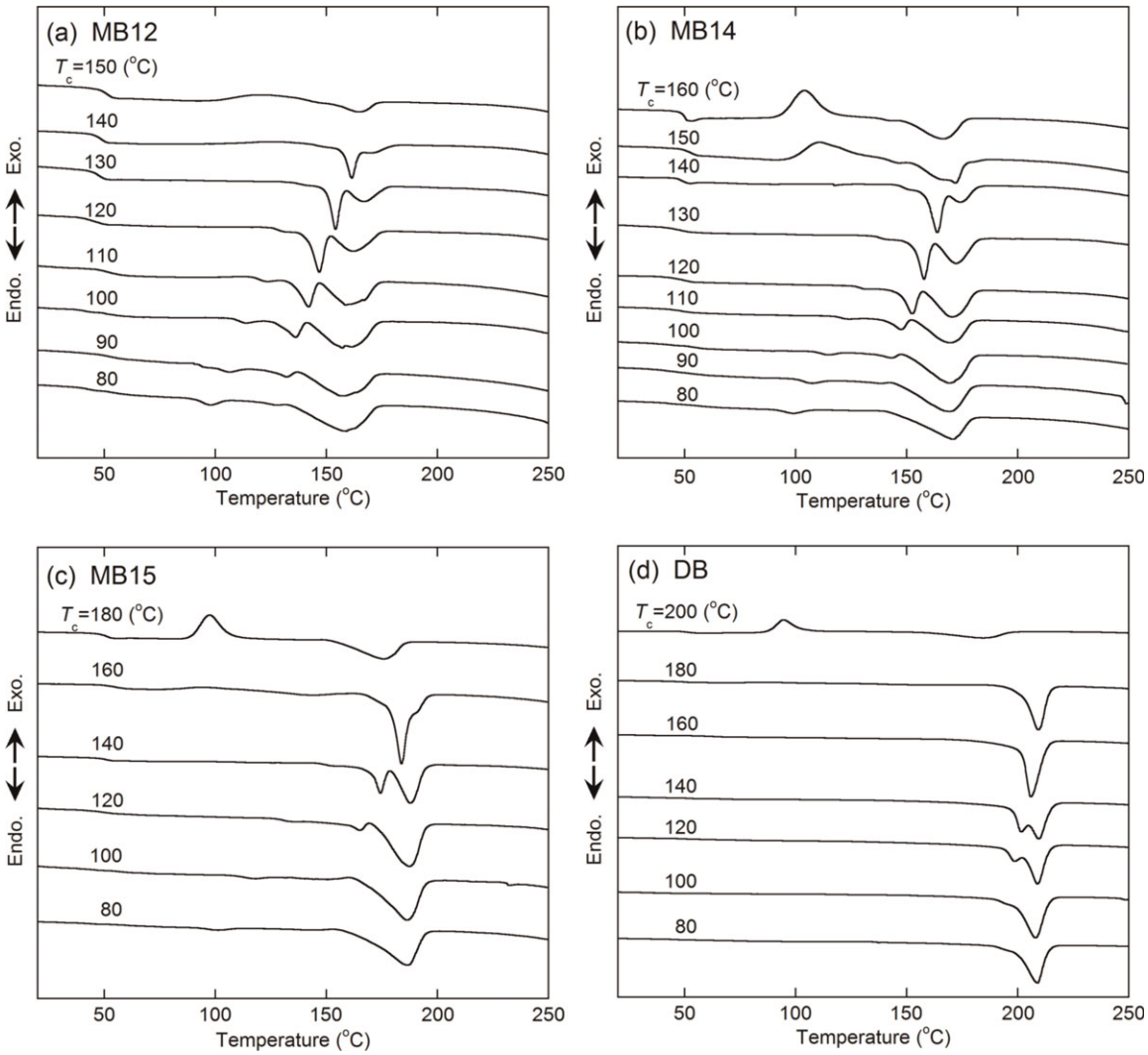

Figure 4. DSC thermograms of polymers and blend isothermally crystallized from the melt at different T_cs.

PLAs and diblock copolymer DB (33–61%) became higher with increasing the block length and were lower than that of the blend L62P/D62P (67%).

Differential Scanning Calorimetry

To monitor the thermal properties of the specimens, DSC was carried out. Figure 4 shows the DSC thermograms of the polymers and blend crystallized at different T_cs. The glass transition and cold crystallization were observed in the ranges of 35–50°C and 85–132°C, respectively. The melting peaks of stereocomplex crystallites of the stereo multiblock PLAs were seen in the wide range of 100–200°C, whereas those of DB and L62P/D62P were observed at around 210 and 230°C, respectively. On the other hand, the melting peak of homo-crystallites of homopolymers L62P and D62P, were seen at around 170°C. The melting temperature (T_m) and total enthalpy of melting and cold crystallization ($\Delta H_m + \Delta H_{cc}$) of polymers and blend were estimated from the DSC thermograms Figure 4 are plotted in Figure 5 as a function of T_c. Here T_m is defined as the peak temperature of T_c-sensitive peak. Most T_m values increased with an increase in T_c and gave maximum values and decreased when T_c approached T_m. The T_m values of stereo multiblock and diblock PLAs increased with increasing block length but lower than that of L62P/D62P. The T_m values of MB15 were higher than or comparable with those of L62P and D62P, whereas those of MB14 and MB12 were lower than or comparable with those of L62P and D62P. This can be ascribed to the fact that shorter block lengths reduced the stereocomplex crystalline thicknesses. The T_c-sensitive T_m is expected to reflect the crystalline sizes depending on T_c, although the multiple melting peaks at higher temperature was probably caused by the melting of imperfect crystallites and subsequent recrystallization. Therefore, we performed the Hoffman–Weeks plot of T_m values in the T_c ranges = 90−130°C for MB12, 100−140°C for MB14, 110−150°C for MB15, 120−170°C for DB, 100−140°C for L62P, 100−150°C for D62P, and 130−170°C for L62P/D62P, respectively (Figure 6). The equilibrium melting temperature (T_m^0) values of stereocomplex crystallites obtained for the stereo multiblock PLAs MB12, MB14, MB15, and the stereo diblock PLA DB were 182.0, 188.4, and 197.7, and 216.5°C, respectively, which were lower than the T_m^0 value 246.0°C of the blend L62P/D62P. As shown in Figure 7, the T_m^0 values of stereocomplex crystallites

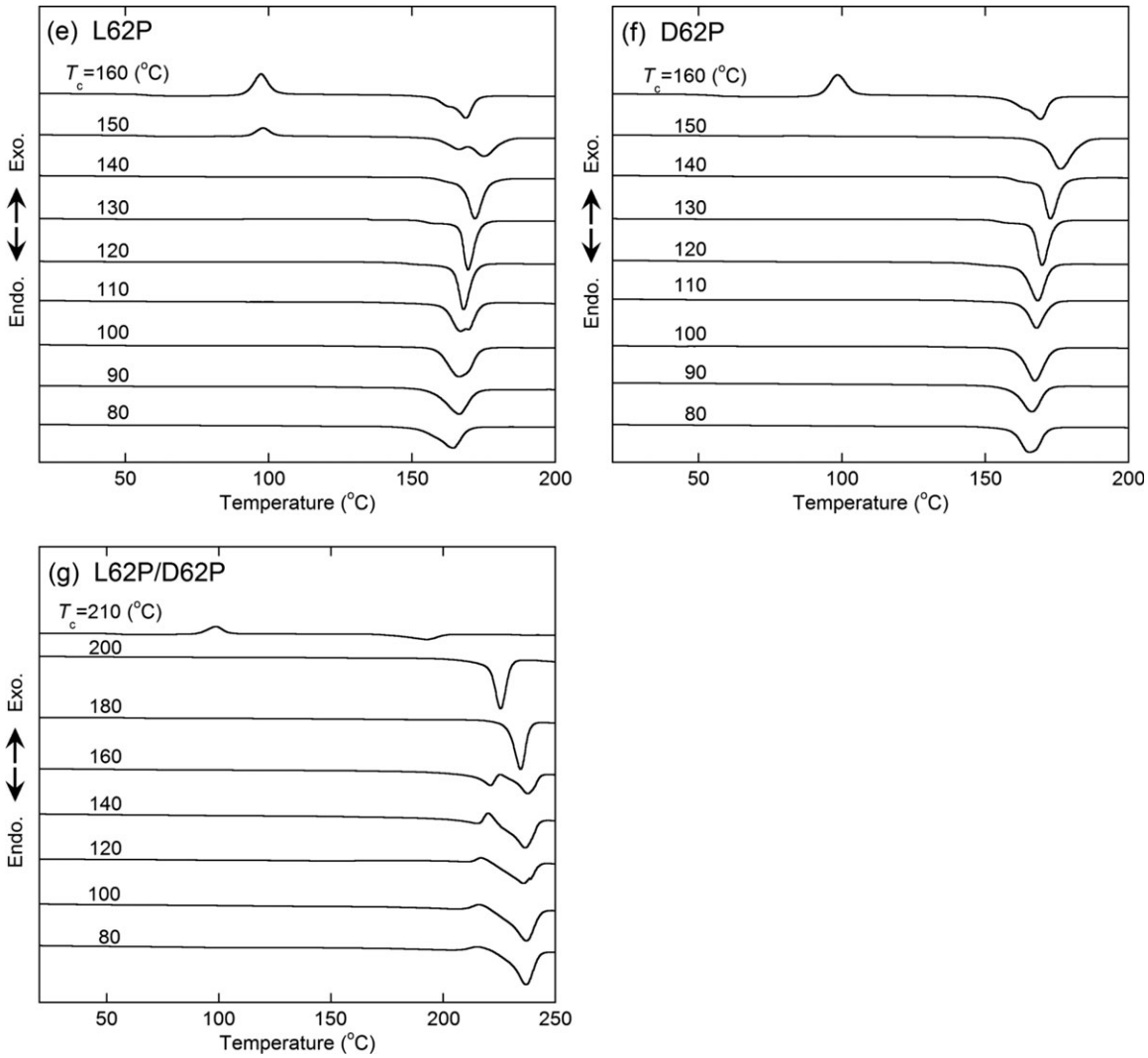

Figure 4. (*Continued*).

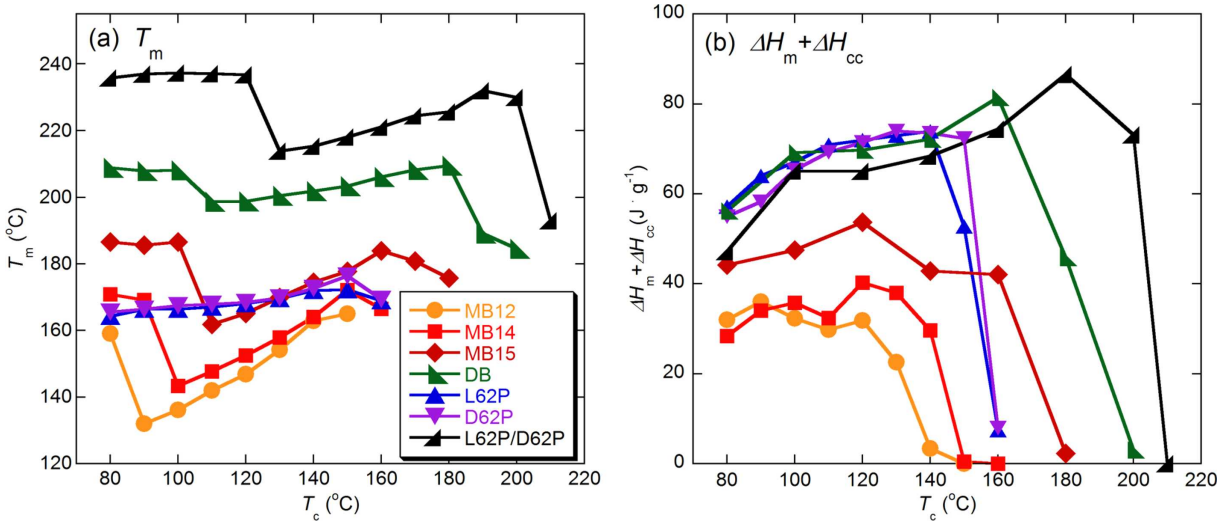

Figure 5. T_m (a) and $\Delta H_m + \Delta H_{cc}$ (b) of polymers and blend isothermally crystallized from the melt at different T_cs. [Color figure can be viewed in the online issue, which is available at wileyonlinelibrary.com.]

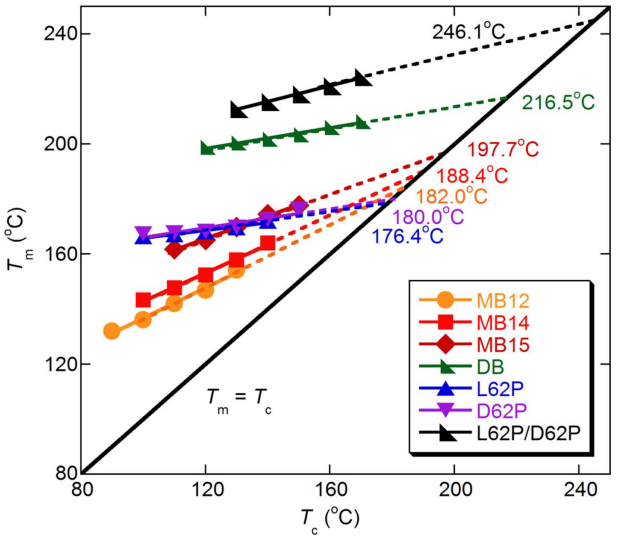

Figure 6. Hoffman–Weeks plot of polymers and blend. [Color figure can be viewed in the online issue, which is available at wileyonline library.com.]

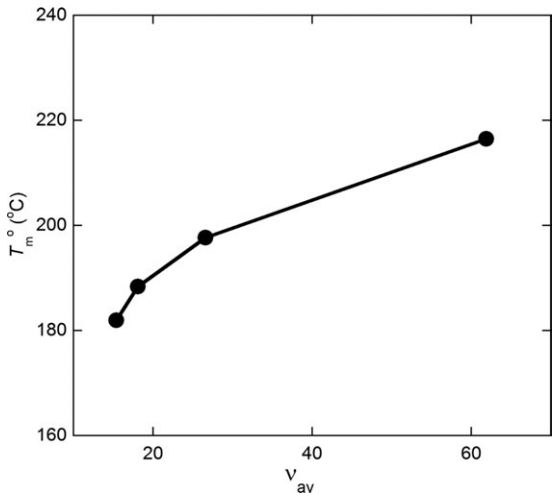

Figure 7. Equilibrium melting temperature (T_m^0) of isothermally crystallized stereo block PLAs as a function of average block length of the L-lactyl and D-lactyl units (v_{av}).

increased with increasing block lengths of PLLA and PDLA. The T_m^0 values of homo-crystallites in L62P and D62P were 176.4 and 180.0°C, respectively. The T_m^0 values of homo-crystallites in the neat L62P and D62P and of stereocomplex crystallites in DB are respectively comparable with those in neat PLLA and PDLA (164.6–188.8°C) and those in stereo diblock polymers (206.3−235.4°C) reported by Tsuji et al.[17] The T_m^0 value of L62P/D62P is much lower than that of reported value for PLLA/PDLA (279°C)[32] but comparable with our previously reported values of stereocomplex crystallities at an infinite molecular weight (241°C) and of stereocomplex crystalline residues as extended chain crystallites formed by hydrolytic degradation (233–237°C).[33]

Overall Crystallization Behavior

The overall crystallization behavior of the polymers and blend at different T_cs were estimated by the time change isothermally crystallized in the light intensity transmitted through the specimens (I) using the polarized optical microscope. The I values increase with an increase in crystallinity and finally levels off when crystallization completes. We used the I defined by the following equation as an index of relative crystallinity (X_r):[34,35]

$$X_r\ (\%) = 100(I_t - I_0)/(I_\infty - I_0), \tag{5}$$

where I_t and I_0 are the I values at crystallization time (t_c) $= t$ and 0, respectively, and I_∞ is the I value when it leveled off.

Figure 8(a,b) shows the relative crystallinity (X_r) of MB15, DB, and L62P/D62P at 160°C and MB12, MB14, MB15, L62P and

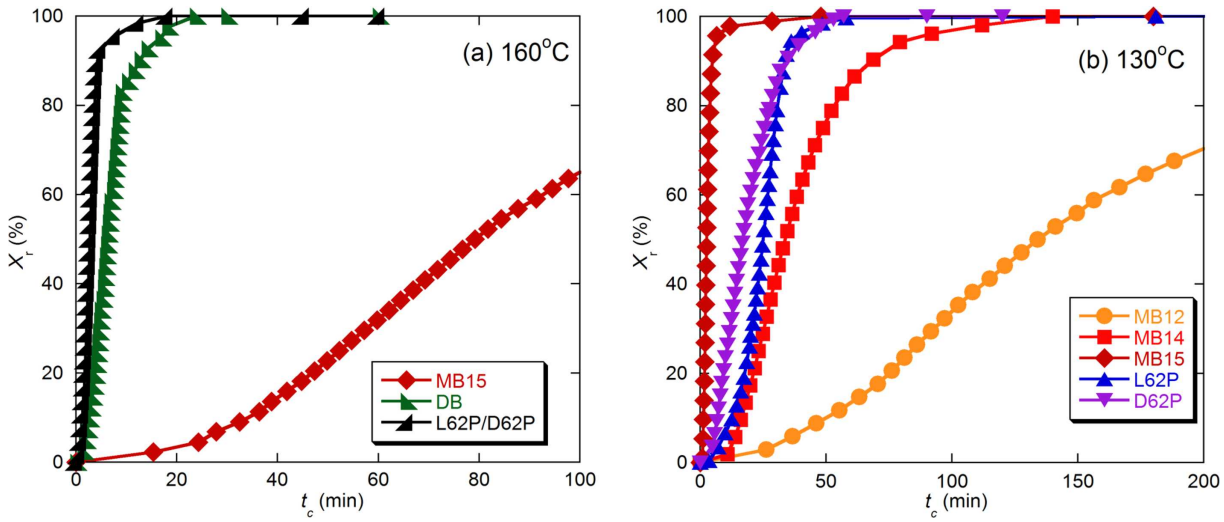

Figure 8. Relative crystallinity (X_r) of MB15, DB, and L62P/D62P (a) and MB12, MB14, MB15, L62P, and D62P (b) isothermally crystallized from the melt at 160°C (a) and 130°C (b), respectively. [Color figure can be viewed in the online issue, which is available at wileyonlinelibrary.com.]

Applied Polymer SCIENCE

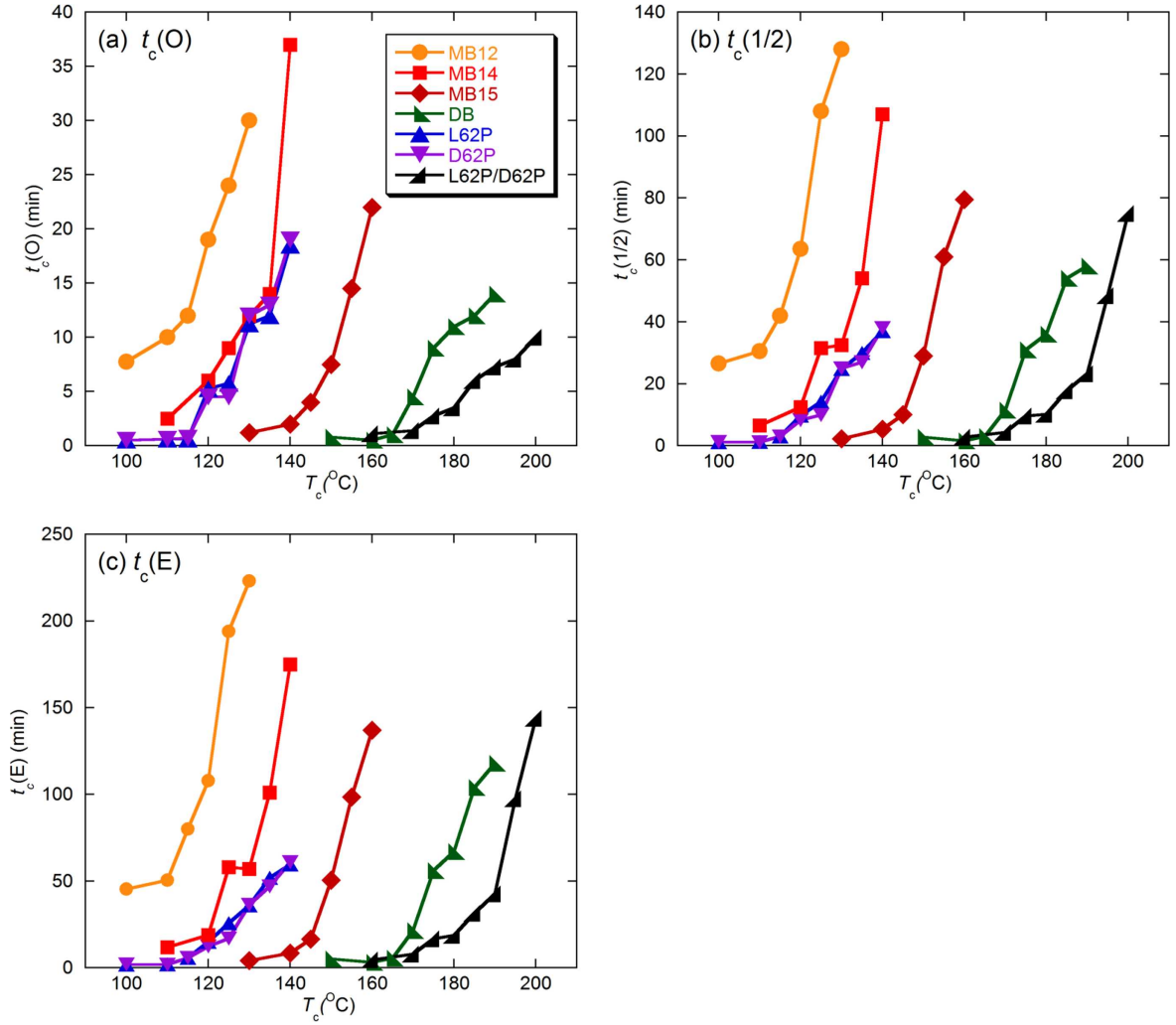

Figure 9. Onset, half and endset times [t_c(O) (a), t_c(1/2) (b), and t_c(E) (c)] of polymers and blend for overall crystallization from the melt at different T_cs. [Color figure can be viewed in the online issue, which is available at wileyonlinelibrary.com.]

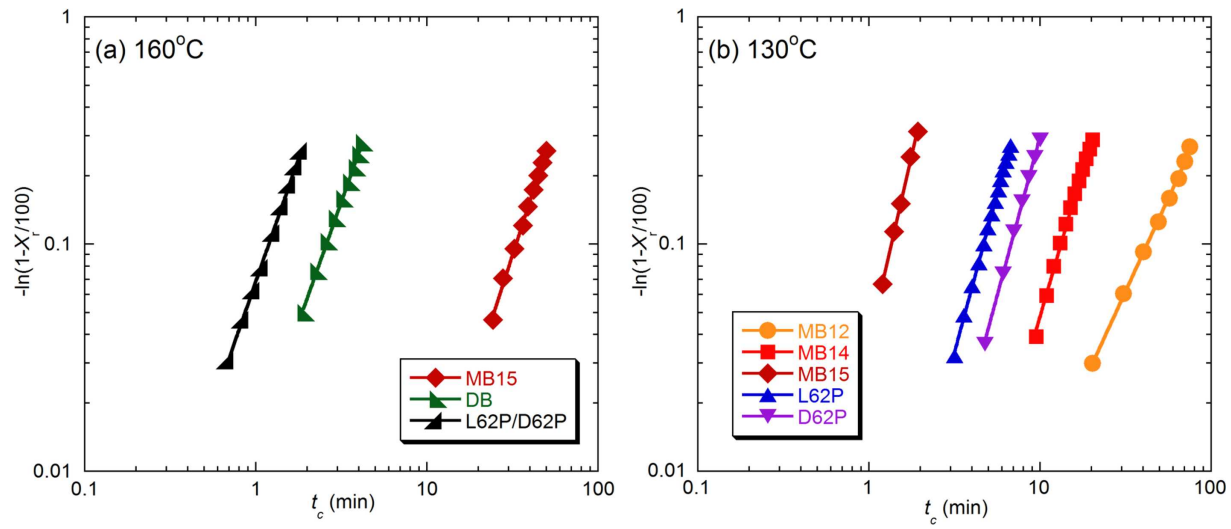

Figure 10. –ln(1 − X_t/100) of MB15, DB, and L62P/D62P (a) and MB12, MB14, MB15, L62P, and D62P (b) isothermally crystallized from the melt at 160°C (a) and 130°C (b), respectively as a function of crystallization time (t_c). [Color figure can be viewed in the online issue, which is available at wileyonlinelibrary.com.]

Table IV. The Avrami Exponent (n) and the Crystallization Rate Constant (k) of Polymers and Blend Crystallized at Different T_cs with their Correlation Coefficient (R^2) and Conversion Range Used for the Fitting Procedure

Code	T_c [°C]	n	n_{av}	k [min^{-n}]	t_c (1/2) [min]	t_c (1/2) (Cal.)[a] [min]	R^2	Conversion range (%)
MB12	100	2.42	2.33	3.01×10^{-4}	26.5	24.5	0.9986	6-22
	110	3.07		2.87×10^{-5}	30.5	26.8	0.9983	5-25
	115	3.25		6.33×10^{-6}	42.0	35.5	0.9996	5-24
	120	1.92		2.20×10^{-4}	63.5	66.3	0.9986	5-23
	125	1.65		2.86×10^{-4}	108.0	112.5	0.9982	6-22
	130	1.64		2.16×10^{-4}	128.0	137.4	0.9987	5-24
MB14	110	2.87	2.71	4.00×10^{-3}	6.5	6.0	0.9987	6-25
	120	3.65		8.52×10^{-5}	12.5	11.8	0.9985	5-24
	125	2.54		1.34×10^{-4}	31.5	29.0	0.9981	5-23
	130	2.44		1.94×10^{-4}	32.5	28.6	0.9983	5-23
	135	2.59		2.98×10^{-5}	54.0	48.5	0.9995	6-23
	140	2.19		2.25×10^{-5}	107.0	112.0	0.9997	6-24
MB15	130	3.40	2.59	3.58×10^{-2}	2.2	2.4	0.9981	6-25
	140	2.71		8.57×10^{-3}	5.3	5.1	0.9998	5-25
	145	2.84		1.23×10^{-3}	10.0	9.3	0.9996	5-25
	150	2.25		3.78×10^{-4}	29.0	28.2	0.9996	6-25
	155	2.07		1.54×10^{-4}	61.0	58.2	0.9998	6-24
	160	2.25		3.87×10^{-5}	79.5	77.7	0.9983	5-23
DB	150	1.87	2.25	8.89×10^{-2}	2.8	3.0	0.9997	5-25
	160	2.12		1.33×10^{-2}	2.6	6.5	0.9987	5-25
	165	2.52		5.50×10^{-2}	3.0	2.7	0.9990	5-24
	170	1.73		1.20×10^{-2}	11.5	10.4	0.9997	5-25
	175	2.37		1.62×10^{-4}	31.0	34.1	0.9991	5-25
	180	2.86		3.72×10^{-5}	36.0	31.1	0.9976	5-24
	185	2.22		1.41×10^{-4}	54.0	46.1	0.9985	5-24
	190	2.29		8.36×10^{-5}	58.0	51.4	0.9979	5-24
L62P	100	2.70	3.14	4.32×10^{-1}	1.1	1.2	0.9989	5-23
	110	4.80		6.19×10^{-1}	1.3	1.0	0.9982	5-24
	115	3.96		8.72×10^{-2}	3.0	1.7	0.9985	5-23
	120	3.71		1.06×10^{-4}	9.8	10.7	0.9990	5-24
	125	2.61		8.25×10^{-4}	14.3	13.2	0.9991	6-24
	130	2.80		1.33×10^{-3}	24.8	9.3	0.9993	4-24
	135	2.13		5.42×10^{-4}	30.0	28.7	0.9987	5-23
	140	2.41		9.61×10^{-5}	37.0	39.9	0.9984	5-23
D62P	100	2.58	2.84	1.13×10^{-0}	1.2	0.8	0.9979	5-23
	110	4.75		3.91×10^{-1}	1.1	1.1	0.9995	4-23
	115	3.21		9.46×10^{-3}	3.0	3.8	0.9986	5-24
	120	3.13		4.71×10^{-4}	8.3	10.3	0.9984	5-24
	125	2.22		2.53×10^{-3}	9.9	12.5	0.9998	5-25
	130	2.40		1.37×10^{-3}	25.0	8.3	0.9998	5-24
	135	1.97		1.36×10^{-3}	27.0	23.7	0.9976	5-23
	140	2.42		8.70×10^{-5}	38.0	40.9	0.9977	5-23
L62P/D62P	160	2.11	1.97	6.92×10^{-2}	2.8	3.0	0.9993	4-24
	170	1.95		3.37×10^{-2}	4.3	4.7	0.9985	5-24
	175	1.84		9.75×10^{-3}	9.6	10.1	0.9983	5-24
	180	2.49		2.26×10^{-3}	10.2	10.0	0.9996	4-25
	185	2.09		1.58×10^{-3}	17.8	18.4	0.9994	4-25
	190	1.77		2.45×10^{-3}	23.3	24.2	0.9995	5-25
	195	1.64		1.22×10^{-3}	48.5	47.8	0.9993	5-24
	200	1.85		3.35×10^{-4}	75.0	61.9	0.9978	5-23

[a]The values were estimated from eq. (8).

Applied Polymer SCIENCE

D62P at 130°C, respectively, as a function of t_c. The onset, half, and endset times [t_c(O), t_c(1/2), and t_c(E), respectively] for overall crystallization are defined and estimated as reported previously.[34,35] These values are plotted in Figure 9 as a function of T_c. The t_c(O), t_c(1/2), and t_c(E) values increased in the following order: blend < diblock PLA < multiblock PLAs and those of multiblock PLAs increased with a decrease in the block length. The t_c(O), t_c(1/2), and t_c(E) values of L62P and D62P were similar to those of MB14. This indicates rapid the crystallization of MB14, despite of its low block lengths compared with those of L62P and D62P.

Isothermal crystallization kinetics traced by light intensity measurement was analyzed with the Avrami theory,[36–38] which is expressed by the following equation:

$$1 - X_r\ (\%)/100 = \exp\ (-kt_c^{\,n}), \tag{6}$$

where k is the crystallization rate constant. Equation (6) can be transformed to eq. (7):

$$\ln[-\ln\ (1 - X_r/100)] = \ln\ k + n\ \ln\ t_c. \tag{7}$$

To avoid deviation from the theoretical curves, as stated by Mandelkern and Lorenzo et al.,[39,40] we used X_r in the range of 5−25% for estimating n and k. The plots with eq. (7) give n as slope and intercept ln k (Figure 10). Thus obtained n and k values are listed in Table IV. The n values were in the ranges = 1.64−3.25 for MB12, 2.19−3.65 for MB14, 2.07−3.40 for MB15, 1.73−2.86 for DB, 2.13−4.80 for L62P, 1.97−4.75 for D62P, and 1.64−2.49 for L62P/D62P, respectively. The average n (n_{av}) values of homopolymers (3.14, 2.84) were higher than those of stereoblock PLAs (2.33−2.71) and blend (1.97). The difference between the highest and lowest n values of stereoblock PLAs MB12, MB14, MB15, and DB, homopolymers L62P and D62, and blend L62P/D62P were 1.61, 1.46, 1.33, 1.13, 2.67, 2.78, and 0.85, respectively, these difference decrease with increasing v_{av} and were higher for homopolymers than those of stereoblock PLAs and blend. The large differences between the highest and lowest n values indicate differences in morphology and crystallization growth mechanism at different T_cs. The n values depend on T_c and tend to have lower values with increasing T_c, in agreement with the reported results.[35,41] As reported elsewhere, in the case of sporadic nucleation with n values of 2, 3, 4, and 6 or higher, the crystalline growth units formed are a fibril, a disc, spherulites, and a sheaf, respectively.[35] The n values of the polymers and blend were in the range of 2–5. The n values depend on the polymer type, blending, crystalline type, and T_c, indicating that the growth units of the polymers and blend depend on these factors.

The t_c(1/2) for crystallization was calculated using the following equation:

$$t_c(1/2)\ (\text{Cal.}) = [(\ln\ 2)/k]^{1/n}. \tag{8}$$

The values of t_c(1/2) (Cal.) thus obtained are summarized in Table IV. The values of t_c(1/2) (Cal.) agree with t_c(1/2) values.

Polarized Optical Microscopy

To investigate the isothermal crystallization behavior in detail, the spherulite growth behavior was monitored by polarized optical microscope. Polarized optical photomicrographs of polymers and blend isothermally crystallized at similar ΔT ($=T_m^{\,0} - T_c$) are shown in Figure 11. The spherulite number per unit area decreased in the following order: stereo multiblock PLAs > stereo diblock PLA > blend. MB15 had the highest spherulite number per unit area; interestingly this indicates that the medium stereo block length around 27 enhances the formation of nuclei of stereocomplex crystallites. Well-defined Maltese crosses were observed for all the samples; this reflects that the crystalline species and the block length did not affect the orientation of lamellae.

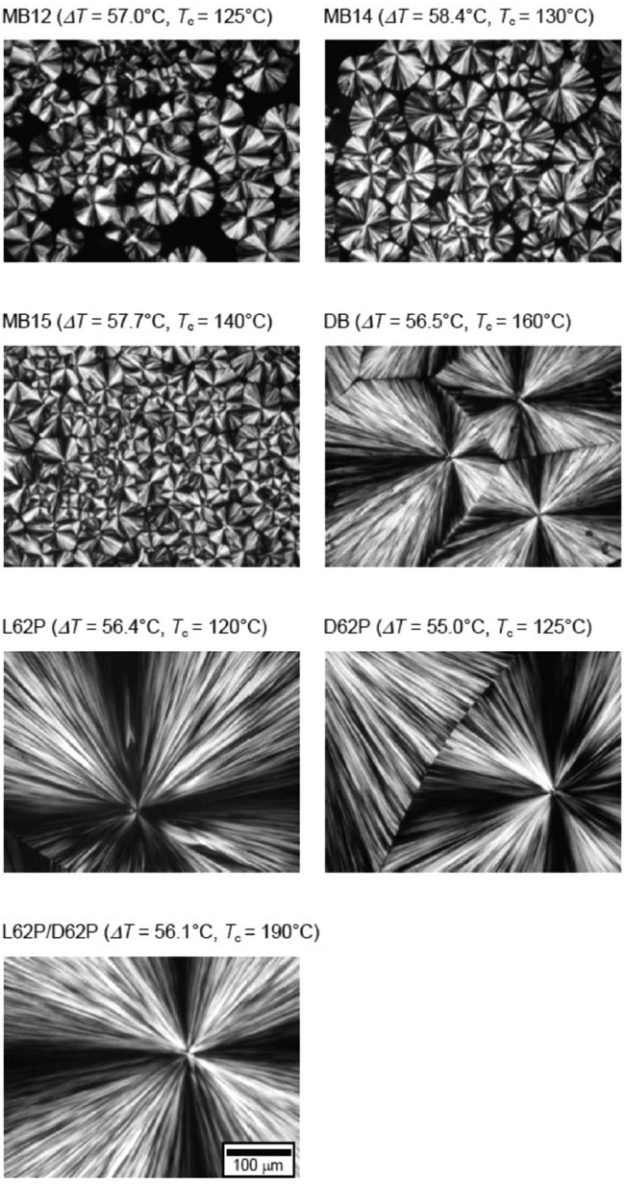

Figure 11. Polarized optical micrographs of polymers and blend isothermally crystallized at similar ΔT.

Spherulite Growth

The radial growth rate of the spherulites (G) and induction period for the spherulite growth (t_i) of the polymers and blend were estimated from the polarized optical photomicrographs

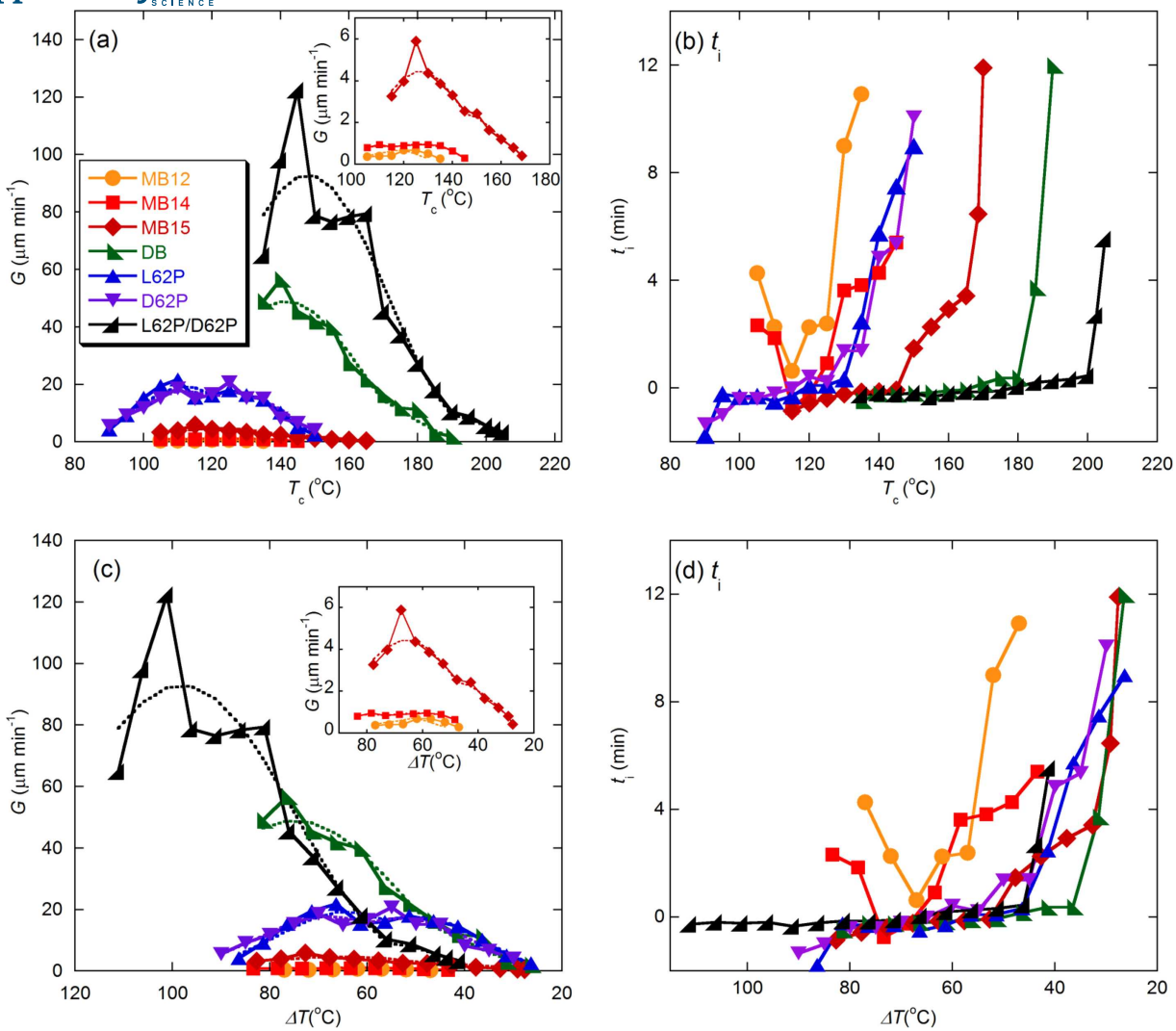

Figure 12. Radial growth rate of spherulites (G) (solid and dotted lines represent measured and calculated G values, respectively) (a,c) and induction period for spherulite growth (t_i) (b,d) of polymers and blend crystallized from the melt as functions of T_c (a,b) and ΔT ($\Delta T = T_m^0 - T_c$, where T_m^0 values were those obtained in Figure 6) (c,d). [Color figure can be viewed in the online issue, which is available at wileyonlinelibrary.com.]

taken at different crystallization times. Thus, the obtained G and t_i values are plotted in Figure 12 as a function of T_c and ΔT ($\Delta T = T_m^0 - T_c$, where T_m^0 values were those obtained in Figure 6). As shown in the Figure 12(a,c), the G values of the stereo multiblock and diblock PLAs increased with increasing block length and the G values of the stereo multiblock PLAs were much lower than those of the homopolymers L62P and D62P, stereo diblock PLA DB, and blend L62P/D62P. The maximum G (G_{max}) values of MB12, MB14, and MB15 were 0.7, 0.9, and 5.0 μm min^{-1}, respectively, which were much lower than those of L62P (17.9 μm min^{-1}), D62P (20.7 μm min^{-1}), DB (56.7 μm min^{-1}), and L62P/D62P (122.5 μm min^{-1}). As shown in Figure 13, the G_{max} values increased with increasing block length of stereoblock PLAs. The G_{max} values decreased in the following order: blend > diblock PLA > multiblock PLA. The former trend is consistent with that in the previous report.[17] As seen in Figure 12(b,d), the t_i values of MB12 and MB14 were practically zero and minima at T_c around 120°C and increased with the deviation of T_c from 120°C. The t_i values of MB15, DB, and L62P/D62P were practically zero in T_c ranges = 115–145, 135–180, and 135–200°C and increased for

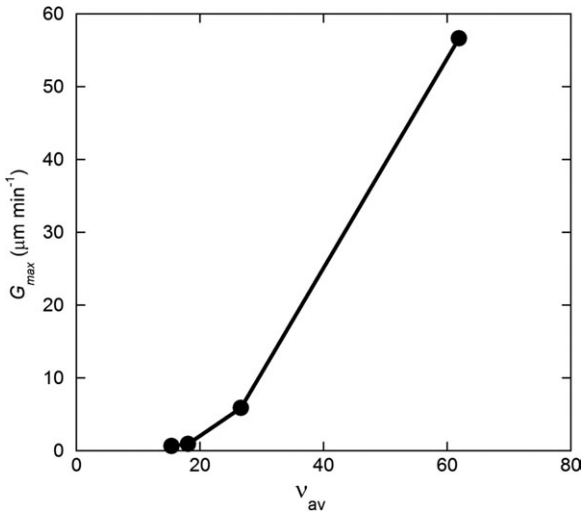

Figure 13. Maximum G (G_{max}) values of stereo block PLAs during isothermal crystallization as a function of average block length of the L-lactyl and D-lactyl units (ν_{av}).

Applied Polymer SCIENCE

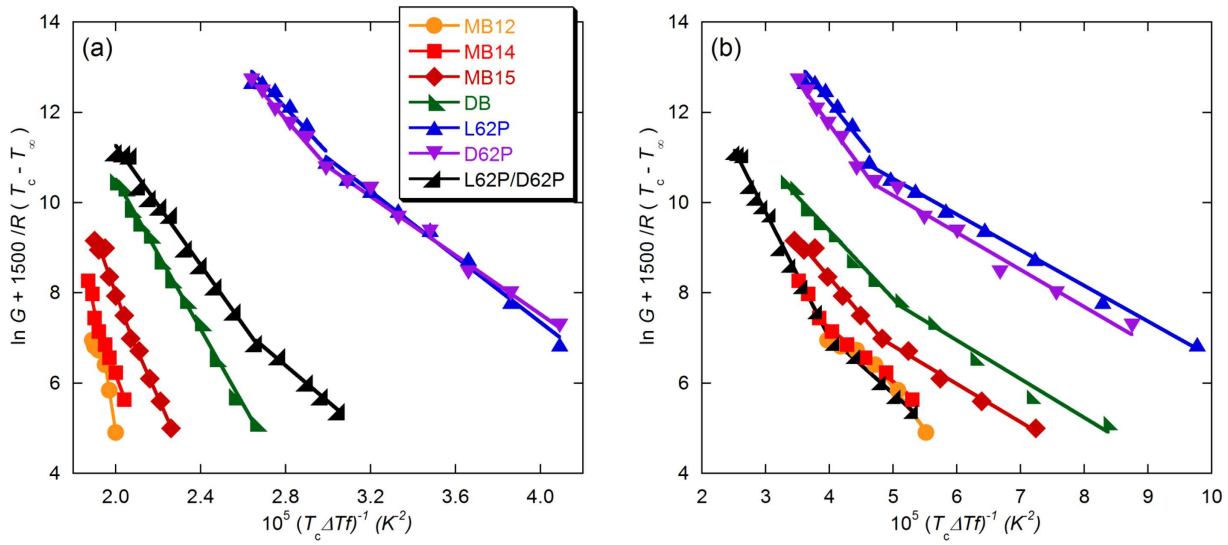

Figure 14. $\ln G + 1500/R(T_c - T_\infty)$ of polymers and blend for fixed and each T_m^0 values (b) as a function of $1/(T_c\Delta Tf)$. [Color figure can be viewed in the online issue, which is available at wileyonlinelibrary.com.]

T_c above 145, 180, and 200°C, respectively. This means that the T_c range of the stereo multiblock and diblock PLAs and blend wherein t_i is practically zero became wider with increasing the block length. The t_i values of L62P and D62P showed similar trend with those of MB14 but were practically zero for the T_c range = 90–130°C.

Hoffman Analysis

The nucleation constant (K_g) and the front constant (G_0) of the specimens were determined using a nucleation theory established by Hoffman et al.,[42] where growth rate (G) data were expressed by the following equation:

$$G = G_0 \exp[-U^*/R(T_c - T_\infty)] \exp[-K_g/(T_c\Delta Tf)] \quad (9)$$

where ΔT is supercooling $T_m^0 - T_c$ when T_m^0 is equilibrium T_m, f is the factor expressed by $2T_c/(T_m^0 + T_c)$ that accounts for the change in the heat of fusion as the temperature is decreased below T_m^0, U^* is the activation energy for the transportation of segments to the crystallization site, R is the gas constant, and T_∞ ($=T_g - 30$K) is the hypothetical temperature where all motion associated with viscose flow ceases.[24,43,44] Figure 14 illustrates the $\ln G + 1500/R(T_c - T_\infty)$ of the polymers and blend as a function of $1/(T_c\Delta Tf)$. Some reported articles used each T_m^0 which varies depending on molecular weight and comonomer type and content.[17,45] We used T_m^0 of each specimen obtained from Hoffman–Weeks procedure (Figure 6) and reported T_m^0 values of homo-crystallites and stereocomplex

Table V. Estimated Front Constants (G_0) and Nucleation Constant (K_g) Values for Fixed and Each T_m^0 Values

	For fixed T_m^0 value			For each T_m^0 value[a]		
Code	G_0 [μm min^{-1}]	K_g [K^2]	Regime	G_0 [μm min^{-1}]	K_g [K^2]	Regime
MB12	1.14×10^{10}	8.58×10^5	II	1.67×10^4	6.92×10^4	II
	1.93×10^{22}	3.01×10^6	I	4.67×10^6	1.88×10^5	I
MB14	5.76×10^{22}	2.36×10^6	III	3.63×10^7	2.59×10^5	III
	3.30×10^{13}	1.26×10^6	II	1.61×10^5	1.19×10^5	II
MB15	7.11×10^{14}	3.31×10^6	III	3.14×10^6	1.19×10^5	III
	4.55×10^{12}	1.07×10^6	II	6.42×10^4	8.48×10^4	II
DB	6.31×10^{11}	8.32×10^5	II	4.90×10^6	1.51×10^5	III
				1.75×10^5	8.54×10^4	II
L62P	3.77×10^{11}	5.20×10^5	III	2.39×10^8	1.76×10^5	III
	4.06×10^9	3.70×10^5	II	1.95×10^6	7.90×10^4	II
D62P	2.37×10^{11}	5.12×10^5	III	2.70×10^8	1.92×10^5	III
	1.04×10^9	3.31×10^5	II	1.60×10^6	8.25×10^4	II
L62P/D62P	4.35×10^{10}	6.61×10^5	III	7.68×10^7	2.79×10^5	III
	4.06×10^7	3.97×10^5	II	1.80×10^5	1.27×10^5	II

[a] T_m^0 values obtained by the Hoffmann-Weeks procedure from Figure 6.

crystallites (212 and 279°C, respectively).[32,46] The T_g values were those of the melt quenched specimens.

The plots in this figure gives K_g values as slopes and intercepts as ln G_0. Thus, the estimated values are given in the Table V. The G values calculated from obtained K_g and G_0 values are shown as dotted lines in Figure 12(a,c). The correspondence between the theoretical and experimental data reveals the validity of the analysis. From the K_g values, we can obtain information about the crystalline growth mechanism. Normally, crystalline growth mechanisms are classified into three regimes, i.e., Regimes I, II, and III, depending on T_c and consequently on the ratio of the lateral growth rate (g) to the rate of formation of secondary nuclei (i). The ratio of g to i increases with an increase in T_c. Regimes I, II, and III are respectively observed for high, middle, and low T_c.

For a fixed T_m^0 values the plots of ln $G + 1500/R(T_c - T_\infty)$ for the stereo multiblock PLAs MB12, MB14, MB15 and those of the homopolymers L62P, D62P, and blend L62P/D62P were composed of two lines. The lines having high and low slopes are assumed for Regime III and II kinetics, respectively (only in the case of MB12 high and low slopes were for Regime I and II kinetics, respectively). This assumption is validated because K_g in Regime I and III kinetics is double that in Regime II kinetics. Stereo diblock PLA DB was composed of one line which is assumed for Regime II kinetics because the K_g value is similar to those of stereo multiblock PLAs for Regime II kinetics. The K_g values in Regime II kinetics of the stereo multiblock and diblock PLAs (8.32×10^5–1.26×10^6 K^2) were higher than those of the blend L62P/D62P (3.97×10^5 K^2). This suggests that the crystallization of stereo multiblock PLAs proceed with different crystallite growth mechanism. The G_0 values in Regime II of the stereo multiblock and diblock PLAs (1.14×10^{10}–3.30×10^{13} μm min^{-1}) were higher than those of the blend L62P/D62P (4.06×10^7 μm min^{-1}). The G_0 values in Regime II of DB (6.31×10^{11} μm min^{-1}) is comparable with reported for stereo diblock PLA (2.31×10^{12} μm min^{-1}) of similar molecular weight ($M_w = 1.32 \times 10^4$).[16] The K_g (5.20×10^5 K^2) and G_0 (3.77×10^{11} μm min^{-1}) values in Regime III of L62P were higher than those of reported K_g (4.60×10^5 K^2) and G_0 (1.19×10^{11} μm min^{-1}) values of PLLA with similar molecular weight ($M_w = 1.20 \times 10^4$ g mol^{-1}).[47]

For each T_m^0 values, the plots of ln$G + 1500/R(T_c - T_\infty)$ for all the synthesized polymers and blend were composed of two lines. The K_g and G_0 values of the synthesized polymers and blend for each T_m^0 value were similar to those for fixed the T_m^0 value. The K_g values for Regime II kinetics were lower for each T_m^0 value (6.92×10^4–1.27×10^5 K^2) than those obtained for the fixed T_m^0 value (8.58×10^5–1.26×10^6 K^2). Also, the G_0 values in Regime II kinetics were lower for each T_m^0 value (1.67×10^4–1.95×10^6 μm min^{-1}) were lower than those obtained for the fixed T_m^0 value (4.06×10^7–3.30×10^{13} μm min^{-1}). The K_g (1.76×10^5 K^2) and G_0 (2.39×10^8 μm min^{-1}) values of L62P in Regime III were higher than reported K_g (8.88×10^4 K^2) and G_0 (1.09×10^7 μm min^{-1}) values of similar molecular weight ($M_w = 1.20 \times 10^4$).[47]

CONCLUSIONS

Only stereocomplex crystallites as crystalline species were formed in stereo multiblock PLAs and DB in isothermal crystallization, irrespective of block length (v_{av} = 15.4–61.9 lactyl units). This indicates that the block copolymerization is very effective method for stereocomplex crystallization. The maximum X_c (33–61%), G_{max} (0.7–56.7 μm min^{-1}), and T_m^0 (182.0–216.5°C) were higher for the stereo multiblock PLAs and diblock PLAs with longer block but were less than those of PLLA/PDLA blend (67%, 122.5 μm min^{-1}, and 246.0°C). The t_c(O), t_c(1/2), and t_c(E) values of the stereo multiblock and diblock PLAs became shorter with increasing the block length and were much longer than those of the PLLA/PDLA blend. The n values of polymers and blend are in the range of 2–5, depending on the polymer type, blending, crystalline type, and T_c. The stereo multiblock and diblock PLAs, neat PLLA, PDLA, and their blend in the present study exhibited Regime III and II kinetics, whereas the stereo mulitblock PLA (MB12) with the smallest v_{av} showed Regime I and II kinetics.

REFERENCES

1. Ikada, Y.; Tsuji, H. *Macromol. Rapid Commun.* **2000**, *21*, 117.
2. Auras, R.; Harte, B.; Selke, S. *Macromol. Biosci.* **2004**, *4*, 835.
3. Seppälä, J. V.; Helminen, A. O.; Korhonen, H. *Macromol. Biosci.* **2004**, *4*, 208.
4. Bendix, D. *Polym. Degrad. Stab.* **1998**, *59*, 129.
5. Rasal, R. M.; Janorkar, A. V.; Hirt, D. E. *Prog. Polym. Sci.* **2010**, *35*, 338.
6. Mecking, S. *Angew. Chem. Int. Ed.* **2004**, *43*, 1078.
7. Rathi, S.; Chen, X.; Coughlin, E. B.; Hsu, S. L.; Golub, C. S.; Tzivanis, M.J. *Polymer* **2011**, *52*, 4184.
8. Gross, R. A.; Kalra, B. *Science* **2002**, *297*, 803.
9. Gupta, A. P.; Kumar, V. *Eur. Polym. J.* **2007**, *43*, 4053.
10. Pan, P.; Inoue, Y. *Prog. Polym. Sci.* **2009**, *34*, 605.
11. Ikada, Y.; Jamshidi, K.; Tsuji, H.; Hyon, S.-H. *Macromolecules* **1987**, *20*, 904.
12. Tsuji, H.; Ikada, Y. *Polymer* **1999**, *40*, 6699.
13. Tsuji, H. *Macromol. Biosci.* **2005**, *5*, 569.
14. Slager, J.; Domb, A. *J. Adv. Drug Delivery Rev.* **2003**, *55*, 549.
15. Yui, N.; Dijkstra P.J.; Feijen, J. *Makromol. Chem.* **1990**, *191*, 481.
16. Bouapao, L.; Tsuji, H. *Macromol. Chem. Phys.* **2009**, *210*, 993.
17. Tsuji, H.; Wada, T.; Sakamoto, Y.; Sugiura, Y. *Polymer* **2010**, *51*, 4937.
18. Othman, N.; Xu, C.; Mehrkhodavandi, P.; Hatzikiriakos, S. G. *Polymer* **2012**, *53*, 2443.
19. Li, L.; Zhong, Z.; de Jeu, W.H.; Dijkstra, P.J.; Feijen, J. *Macromolecules* **2004**, *37*, 8641.
20. Hirata, M.; Kobayashi, K.; Kimura, Y. *J. Polym. Sci. Part A: Polym. Chem.* **2010**, *48*, 794.
21. Michell, R. M.; Müller, A. J.; Spasova, M.; Dubois, P.; Buratttini, S.; Greenland, B. W.; Hamley, I. W.; Hermida-Merino,

D.; Cheval, N.; Fahmi, A. *J. Polym. Sci. Part B: Polym. Phys.* **2011**, *49*, 1397.

22. Castillo, R. V.; Müller, A. *J. Prog. Polym. Sci.* **2009**, *34*, 516.
23. Rahaman, M. H.; Tsuji, H. *Macromol. React. Eng.* **2012**, *6*, 446.
24. Tsuji, H.; Sugiura, Y.; Sakamoto, Y.; Bouapao, L.; Itsuno, S. *Polymer* **2008**, *49*, 1385.
25. Tsuji, H.; Ikada, Y. *Polym. Degrad. Stab.* **2000**, *67*, 179.
26. Tsuji, H.; Del Carpio, C. A. *Biomacromolecules* **2003**, *4*, 7.
27. Fukushima, K.; Furuhashi, Y.; Sogo, K.; Miura, S.; Kimura, Y. *Macromol. Biosci.* **2005**, *5*, 21.
28. Spassky, N.; Wisniewski, M.; Pluta, C.; Borgne, A. L. *Macromol. Chem. Phys.* **1996**, *197*, 2627.
29. Chabot, F.; Vert, M. *Polymer* **1983**, *24*, 53.
30. Kister, G.; Cassanas, G.; Vert, M. *Polymer* **1998**, *39*, 267.
31. Okihara, T.; Tsuji, M.; Kawaguchi, A.; Katayama, K.; Tsuji, H.; Hyon, S. –H.; Ikada, Y. *J. Macromol. Sci. Phys.* **1991**, *B30*, 119.
32. Tsuji, H.; Ikada, Y. *Macromol. Chem. Phys.* **1996**, *197*, 3483.
33. Tsuji, H.; Tsuruno, T. *Polym. Degrad. Stab.* **2010**, *95*, 477.
34. Tsuji, H.; Takai, H.; Saha, S. K. *Polymer* **2006**, *47*, 3826.
35. Tsuji, H.; Yamamoto, S.; Okumura, A. *J. Appl. Polym. Sci.* **2011**, *122*, 321.
36. Avrami, M. *J. Chem. Phys.* **1939**, *7*, 1103.
37. Avrami, M. *J. Chem. Phys.* **1940**, *8*, 212.
38. Avrami, M. *J. Chem. Phys.* **1941**, *9*, 177.
39. Mandelkern, L. Crystallization of Polymers; McGraw-Hill: New York, **1964**.
40. Lorenzo, A. T.; Arnal, M. L.; Albuerne, J.; Müller, A. *J. Polym. Test* **2007**, *26*, 222.
41. Ke, T.; Sun, X. *J. Appl. Polym. Sci.* **2003**, *89*, 1203.
42. Hoffman, J. D.; Frolen, L. J.; Ross, G. S.; Lauritzen, J. I., Jr. *J. Res. Natl. Bur. Stand. Phys. Chem.* **1975**, *79A*, 671.
43. Abe, H.; Harigaya, M.; Kikkawa, Y.; Tsuge, T.; Doi, Y. *Biomacromolecules* **2005**, *6*, 457.
44. Tsuji, H.; Miyase, T.; Tezuka, Y.; Saha, S. K. *Biomacromolecules* **2005**, *6*, 244.
45. Tsuji, H.; Shimizu, K.; Sakamoto, Y.; Okumura, A. *Polymer* **2011**, *52*, 1318.
46. Tsuji, H.; Ikada, Y. *Polymer* **1995**, *36*, 2709.
47. Tsuji, H.; Tezuka, Y.; Saha, S. K.; Suzuki, M.; Itsuno, S. *Polymer* **2005**, *46*, 4917.